Robson, B. E., Collinson, M. E., Riegel, W., Wilde, V., Scott, A. C., & Pancost, R. D. (2015). Early Paleogene wildfires in peat-forming environments at Schöningen, Germany. Palaeogeography, Palaeoclimatology, Palaeoecology, 437, 53-62. DOI: 10.1016/j.palaeo.2015.07.016

Palaeogeography, Palaeoclimatology, Palaeoecology 437 (2015) 53–62

Contents lists available at ScienceDirect

Palaeogeography, Palaeoclimatology, Palaeoecology

journal homepage: www.elsevier.com/locate/palaeo

Early Paleogene wildfires in peat-forming environments at Schöningen, Germany

Brittany E. Robson [a,*], Margaret E. Collinson [a], Walter Riegel [b], Volker Wilde [c], Andrew C. Scott [a], Richard D. Pancost [d]

[a] Department of Earth Sciences, Royal Holloway University of London, Egham, Surrey, TW20 0EX, UK
[b] Geowissenschaftliches Zentrum Göttingen, Geobiologie, Goldschmidtstrasse 3, D-37077, Göttingen, Germany
[c] Sektion Palaeobotanik, Senckenberg Forschungsinstitut und Naturmuseum, Senckenberganlage 25, 60325 Frankfurt am Main, Germany
[d] The Cabot Institute and the Organic Geochemistry Unit, School of Chemistry, University of Bristol, Cantocks Close, Bristol, BS8 1TS, UK

ARTICLE INFO

Article history:
Received 31 March 2015
Received in revised form 7 July 2015
Accepted 10 July 2015
Available online 19 July 2015

Keywords:
Inertinite
Charcoal
Coal
Lignite
Eocene
EECO

ABSTRACT

Wildfire activity in early Paleogene greenhouse conditions can be used as an analogue to gauge the effect of future warming trends on wildfire in the current climate system. Inertinite (fossil charcoal in coal) from 11 autochthonous early Paleogene lignite seams from the Schöningen mine (Germany) was quantified using macerations, *in situ* pillars and industry standard crushed samples. A new three transect method was developed to quantify *in situ* charcoal. The combination of *in situ* pillars and crushed samples accounts for temporal and spatial variation in charcoal through a stratigraphically oriented pillar, whilst maintaining comparability with industry standards and previous work. Charcoal occurs as a range of randomly distributed particle sizes, indicating that fires were burning locally in the Schöningen peat-forming environment and in the surrounding areas, but according to petrological data, not in an episodic or periodic pattern. Although charcoal abundance is low (relative to previous high fire worlds such as the Cretaceous), three quantitative and semi-quantitative methods show increased wildfire activity (relative to the modern world) in the warmest parts of the early Paleogene. As atmospheric oxygen levels stabilised to modern values and precipitation and humidity became the main control on wildfire, increased rainfall followed by drier intervals would have created an environment rich in dry fuel in which wildfires could easily propagate if humidity was low enough. In the later part of the Early Eocene (Ypresian) charcoal abundance fell to levels similar to those found in modern peats. This indicates that the transition to the modern low fire world occurred within the Early Eocene, earlier than previous records suggest.

1. Introduction

Wildfire has always been an important part of the natural environment (Bowman et al., 2009; Pausas and Keeley, 2009; Scott et al., 2014), but the role of wildfire in the early Paleogene ecosystems is not yet fully understood (Scott, 2000; Belcher et al., 2013). One of the key sources of evidence for ancient wildfires is the presence of charcoal (Potonié, 1929; Harris, 1958; Komarek, 1972; Scott, 1989, 2000, 2010; Glasspool and Scott, 2013; Scott et al., 2014), an inert substance with a high potential for survival in the fossil record (Scott, 1989, 2010; Figueiral, 1999). A 400 million year record of charcoal in coals (Glasspool and Scott, 2010; also replotted by Bond, 2015) showed a transition in the Cenozoic from moderate (17% in the Paleocene) to low (3.5% in the Middle to Late Eocene) charcoal percentages. However, that study was limited by the use of 10 million year bins. Paleogene warm climates (e.g. the Early Eocene Climatic Optimum, EECO) are not direct analogues for future warming trends in the current climate system because they occur during a time when global temperatures were significantly warmer than now. However, improved temporal resolution of early Paleogene wildfire activity can lead to better understanding of the modern fire world and contribute to better predictions of wildfire activity in future warm climates.

Charcoal can accumulate in any depositional environment, but peat deposits are particularly valuable archives of past wildfire activity. Peat is an accumulation of partially decayed plant material which, after peatification and burial diagenesis, may transform to lignite. Lignite is less altered than more mature, higher rank, coals, preserving a record of the peat-forming environment and vegetation (Teichmüller, 1989; Scott, 1991a,b; Wüst et al., 2001; Moore and Shearer, 2003) sometimes to the molecular level (Pancost et al., 2007; Fabbri et al., 2009). Charcoal in the peat-forming environment is likely to be preserved closer to its point of formation than in other settings, as it is not subjected to variables of fluvial transport including differential saturation (Vaughan and Nichols, 1995; Nichols et al., 2000), concentration, floatation, size

* Corresponding author at. Earth Sciences, Queens Building, Royal Holloway University of London, Egham Hill, Surrey, TW20 0EX, UK.
E-mail address: Brittany.Robson.2008@live.rhul.ac.uk (B.E. Robson).

http://dx.doi.org/10.1016/j.palaeo.2015.07.016

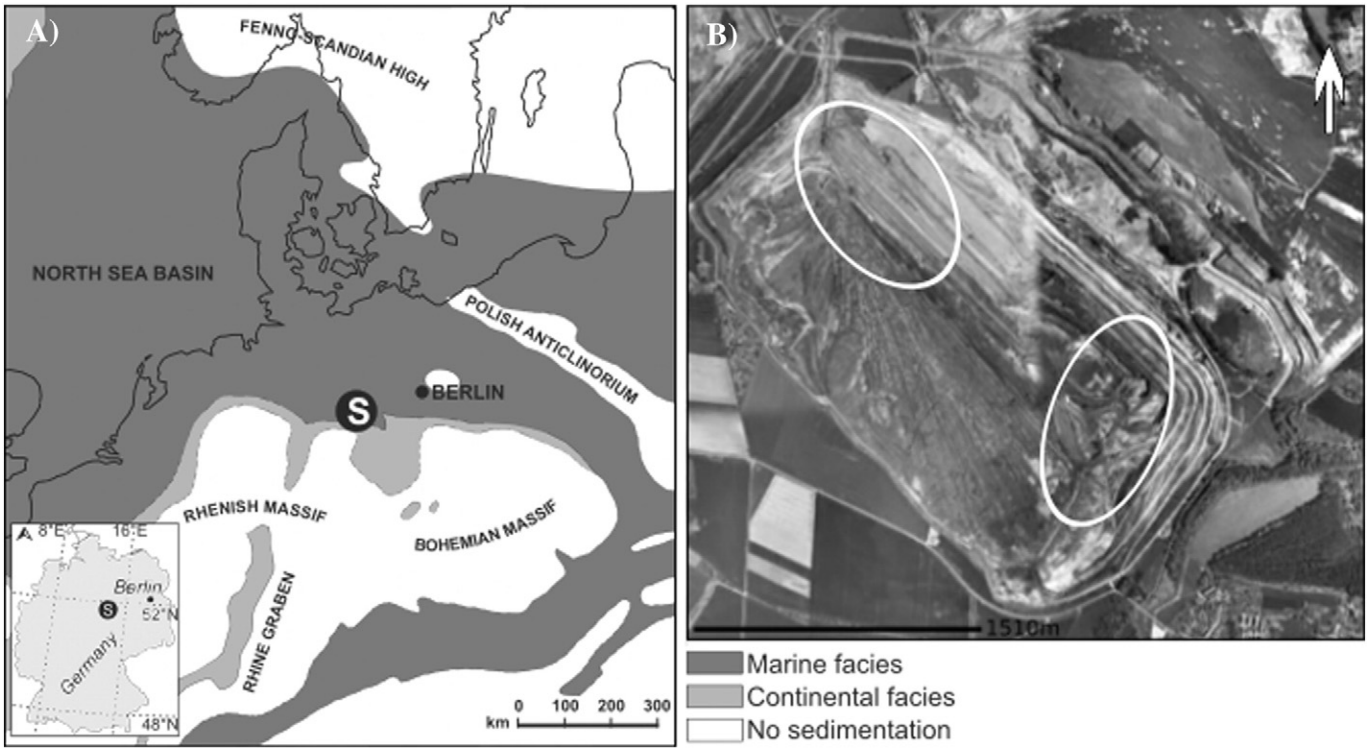

Fig. 1. (A) Central European palaeofacies map showing the location of the Schöningen mine (white S in black circle), modern coastlines and Germany (see inset); modified from Riegel et al. (2015, Fig 1). (B) An overview of the Schöningen mine (Google Earth, accessed September 2013) with approximate collecting areas marked in the north and south.

sorting and fragmentation (Nichols, 1999; Scott et al., 2000). Moreover, peat-forming environments require hydrological stability (Holden, 2005), which mitigates the impact of different climate regimes when comparing records of wildfire (Glasspool and Scott, 2010). Therefore, the charcoal record in lignites offers the best option for comparison of the wildfire record between past time intervals.

Riegel et al. (2012) have undertaken a long term stratigraphic, sedimentological and palaeoenvironmental study of the Schöningen mine (Fig. 1), the sole north German locality where early Paleogene lignites can be studied in succession. Their field surveys document charcoal in multiple seams in different quantities. The current work uses three methods to quantify charcoal in the Schöningen sequence of early Paleogene peat-forming environments, enabling high resolution reconstruction of long term changes in early Paleogene wildfire and interpretation of the timing of the transition to modern levels of fire activity.

2. The Schöningen mine

2.1. Regional geology and palaeoenvironments

The Schöningen Südfeld open cast mine in Lower Saxony, Northern Germany (52.1333° N, 10.9500° E) exposes a sequence of 170 m that includes 11 continuous (occasionally splitting) lignite seams, the oldest (and thickest) of which is Main seam followed by seams 1–9 (supplementary Figs. 1.1 and 1.2). Locally, the lignite seams of minor thickness are intercalated, including "seam L" (between seam 6 and 7, supplementary Fig. 1.1B), which was also sampled for this study. The mine is located on one of the rim synclines of the Helmstedt-Stassfurt salt wall, a prominent structure that runs NW–SE within the Subhercynian basin (Brandes et al., 2012, 2013; Osman et al., 2013) for more than 70 km (Riegel et al., 2012). Rim synclines formed around the domed salt wall (Manger, 1952), and although there is some regional deformation due to the salt dome there is no obvious faulting in the Schöningen area.

Rooting is generally prevalent in nearly all lignite seams at Schöningen and is frequently visible from the lignite beds into the underlying interbeds, indicating autochthonous peat accumulation (supplementary material herein; Riegel et al., 2012). Between each seam is an interbed composed of clastic sediments, these sediments are crucial indicators of the depositional environment (Riegel et al., 2012). Characteristic features include bimodal cross bedding, coarsening and fining upward sequences, *Ophiomorpha* burrows and infilled burrows in tops of seams. Taken together these indicate a nearshore coastal setting subjected to tidal influence, changes in energy regime and episodic submergence or emergence (Riegel et al., 2012). Interbed 5 (above seam 4) also contains rooted seagrasses, which clearly indicate marine influence (supplementary material herein; Riegel et al., 2012). Thick, flat lying root branches immediately underlying seam 6 were interpreted by Riegel et al. (2012) as indication of a tall mire forest growing on a marine substrate. Interbed 9 (above seam 8) shows the least marine influence at Schöningen as indicated by *in situ* palm stumps (supplementary Fig. 2.10.3; Riegel et al., 2012).

Combined evidence from lignite seams and interbeds at Schöningen reveals three main facies. Terrestrial peat-formation is obvious from the many lignite seams, shore-line deposition is indicated by palm stumps and evidence of intertidal sedimentation is visible in most interbeds. It has commonly been suggested that Schöningen was part of an estuarine environment (Standke, 2008; Krutzsch, 2011; Riegel et al., 2012) in which the peat-forming environment was cyclically flooded by marine transgressions. The sequence, therefore, is a suitable study site to examine temporal variations in charcoal occurrence in the peat-forming environments of a low-lying coastal setting.

2.2. Dating

Based on palynology, Pflug (1952) regarded the lower group of lignite seams (Schöningen Formation sensu; Riegel et al., 2012) as Early Eocene and the upper seam group (Helmstedt Formation including the Victoria seam) as Middle Eocene. Lenz (2005) also concluded that the Helmstedt Formation is Middle Eocene based on palynological evidence. The palynology at Schöningen has been well documented by Riegel et al.

(2012) who found that pollen and spore assemblages are very similar in all seams apart from an increase in palm pollen in seam 4.

Evidence for dating the lowest part (Main seam and seam 1) of the Schöningen Formation comes from Ahrendt et al. (1995) who identified dinoflagellate zone D5b, as defined by Köthe (1990), in the interbed directly above Main seam in the opposite syncline in the Emmerstedt area. If the Main seam in the Emmerstedt area is coeval with the Main seam at Schöningen, then this implies that interbed 1 and seam 1 at Schöningen are Early Eocene and the Paleocene–Eocene (Thanetian–Ypresian) boundary would be within Main seam or below. However, it must be noted that the dinoflagellate marker species for base zone D5b (LO *Apectodinium augustum*) is not present in the onshore sections in northern Germany (Köthe, 1990, 2012) and the marker for top zone D5b (FO *Wetzeliella astra*) is very rare (Köthe, 1990). Furthermore Köthe (1990) stated that an *Apectodinium* acme persisted in zone D5b but that zone D5a was absent. By the original definitions (Costa and Manum, 1988) the *Apectodinium* acme occurs in D5a so it is unclear why Köthe (1990) considered D5a to be absent. Köthe (2012 p. 207) stated "the exact position of the *Apectodinium* acme in the study area [German Sector, SE North Sea Basin] has become uncertain".

Although there are few dinoflagellates present in the interbeds at Schöningen, probably due to the nearshore depositional settings, Riegel et al. (2012) recorded an abundance of *Apectodinium* commencing within interbed 2. If this represents the *Apectodinium* acme of zone D5b, and associated with the Paleocene–Eocene thermal maximum, then Main seam, interbed 1, seam 1 and the lowermost part of interbed 2 are Paleocene.

Evidence for dating the top seam in the Schöningen succession also comes from Ahrendt et al. (1995) who identified dinoflagellate zone D9a, as defined by Köthe (1990), in boreholes from the Emmerstedt area at levels both below and above a horizon they correlated with the Emmerstedter Grünsand at the top of the lower seam group. Zone D9a is calibrated to Chron C22r by Gradstein (2012) and is within the late Ypresian. Assuming that the lower seam group in the Emmerstedt and Helmstedt area (some 12 km north east of Schöningen) is coeval with the lower seam group at Schöningen (with the Emmerstedter Grünsand either being missing or replaced by interbed 9 at Schöningen. Riegel et al., 2012) then the uppermost seam (seam 9) studied in this paper is likely to be within the late Early Eocene.

Although there are uncertainties we treat seam 9 as late Early Eocene (Ypresian) in this paper. Based on this, we tentatively suggest that seam 5 was associated with the EECO. Main seam and seam 1 may be either earliest Eocene or latest Paleocene.

3. Methods

3.1. Field collections

Collecting opportunities at Schöningen are dependent on mining activities. In 2012 and 2013 samples were collected specifically for this charcoal study from Main seam to seam 9. All of the samples were collected in the north area of the mine except for seam 9 which was sampled in the south east. Between 2005 and 2010 samples were collected from seams 1 to 9 during the research leading to publication by Riegel et al. (2012). Seam 3 was sampled in both the north and south west areas of the mine. Seams 4 and 6 were sampled in the north area of the mine. Seams 1, 2, 5, L, 7 and 8 were sampled in the south west area of the mine. Seam 9 was sampled in the south east of the mine. The samples collected were archived in the Senckenberg Museum Palaeobotany Section and sub-sampled for use in this study in 2014.

3.2. In situ pillars, crushed blocks and macerations

To preserve intact stratigraphy from various parts of the seam, two adjacent stratigraphically oriented intact lignite pillars were excavated in the field (2012 and 2013 field season only) and tightly wrapped in extra strong aluminium foil to prevent breakage. The supplementary materials show the exact position of pillars within the seams. In the laboratory one pillar was dried and embedded in resin. The impregnated block was then polished following the method of Collinson et al. (2007) to produce an "*in situ* pillar". The second pillar was preserved in cold storage for future subsampling. Bulk samples were collected in the field from each bed within the seam. Beds were defined by a change in lithotype and, for the 2012 and 2013 field seasons, are shown on the logs in the supplementary material. Logs for the 2005–2010 field seasons are archived in the Senckenberg Museum Palaeobotany Section. Samples representing a whole seam or part of a seam (upper/middle/lower), composed of 5 g of each lignite bed, were produced for each seam. The number of parts is based on seam thickness. Thin seams 3, 4, 5, L, 7, 8 and 9 were subdivided into 2 parts (lower and upper); thick seams Main, 6 and 1 were subdivided into 6, 4 and 3 parts respectively. Thicker seams with more beds are therefore represented by a larger whole seam sample and more part seam samples. For example, the 'part seam' sample 32Scho1.XXXIII.2-5 includes samples from each of the beds 2 to 5 as shown on the log of seam 1 (supplementary material Fig 2.2.3). Information on the beds incorporated into each part seam sample can be obtained in this manner using the supplementary material.

Whole and part seam samples were prepared to industry standard by Jim Hower and colleagues at the Centre for Applied Energy Research, University of Kentucky, where possible samples were crushed to the standard 20 mesh size, ≤840 μm, using a grinder. Soft samples were crushed manually to a top particle size of c. 1000 μm. A subsample was embedded in epoxy resin. The resultant small short cylindrical blocks were polished using 60-, 240-, 400-, and 600-grit SiC papers followed by 0.3 micron alumina on Buehler TexMet paper and 0.05 micron alumina on silk. The final product is a polished block (essentially equivalent to a petrographic pellet in some author's terminology) prepared to industry standards containing a crushed lignite sample. The resin embedded crushed samples and *in situ* pillars both allow for repeated or future study of the same sample. Polished blocks containing crushed samples were viewed in reflected light under immersion oil (Cargille type A, density 0.923 g/cc at 23 °C, RI of 1.514) using a Leica reflected light microscope and either ×20 or ×50 oil immersion objectives. Photomicrographs were gathered as colour jpeg using a 5 megapixel ProgRes Capture Pro 2.7 camera.

20 g lignite samples, from the same bed from which each *in situ* pillar was obtained, were treated with 15% H_2O_2 for 4 hours before sieving in water into size factions retained on 125 μm, 250 μm, 500 μm and 1 mm sieve meshes. Particles released were studied using light microscopy suspended in distilled water so as to reduce breakage. Charcoal particle abundance was estimated for the 250–500 μm size fraction. An ACFOR (abundant, common, frequent, occasional, rare) Domin scale, as used in ecology, was modified by combining the abundant and common categories.

3.3. Petrography and inertinite quantification

Some authors separate charcoal into categories based on its perceived origin (Teichmüller, 1989; Moore et al., 1996; Valentim et al., 2013) but this separation has been questioned extensively (Winston, 1993; Scott, 1989, 2000; Scott and Glasspool, 2007). Multiple charring experiments have been performed on various plants and fungi (e.g. Jones et al., 1993, 1997; Guo and Bustin, 1998; McParland et al., 2007; Scott, 2010 and references therein) all of which demonstrate that increasing charring temperature leads to increasing reflectance. In the petrographic study of coals charcoal is referred to as inertinite (ICCP, 1963, 2001; Sýkorová et al., 2005). Increased reflectance (compared to other components) characterises inertinite, thus, in the absence of macrinite, micrinite and secretinite which are restricted to hard coals, charcoal and inertinite can be considered synonymous.

Lignite components, i.e. macerals, were identified according to the International Committee for Coal and Organic Petrology (ICCP) standard allowing for comparability between disciplines and

practitioners. Four inertinite macerals were studied in this paper, fusinite, semifusinite, inertodetrinite and funginite. Fusinite (Fig. 2A–D) has the highest reflectance of the inertinite macerals (ICCP, 2001) so it appears brighter than all of the other macerals under reflected light. Pieces usually show well preserved cellular structure but a homogeneous particle with high reflectance can still be classified as fusinite as decomposition before charring can result in a bright relatively homogenous maceral (Taylor et al., 1998). Semifusinite (Fig. 2B and D) is a product of low temperature charring, consequently it has lower reflectance than fusinite but higher than huminite (ICCP, 2001). Semifusinite particles typically have less clear cellular structure than fusinite particles (ICCP, 2001). Inertodetrinite (Fig. 2C and E) is classified by the ICCP (2001) as a charcoal maceral which is not larger than 10 μm. Particles are formed by desiccation, attrition or crushing of a larger particle (ICCP, 2001). Scott and Glasspool (2007, see also Scott, 2010) argued that fragmentation during combustion forms small ash-like inertinite particles that are often transported by wind and are therefore indicative of regional wildfire activity. Fungal spores and sclerotia (Fig. 2F) are often preserved in lignite. Charred fungal remains are referred to as funginite (previously sclerotinite) (ICCP, 2001). Although not all agree that these remains represent charred material (Hower et al, 2009), it has been proven that reflectance increases with charring temperature in fungal sclerotia (Figs. S14 e and f in Scott et al., 2010 auxiliary material). For the purposes of this study uncharred fungal remains were included in the huminite category.

Inertinite percentages have been obtained from *in situ* pillars and crushed samples representing lignite seams sampled at Schöningen. Previous work has quantified inertinite in *in situ* pillars using eyepiece graticule grids (Belcher et al., 2005; Collinson et al., 2007; Hudspith et al., 2012), but there is no standard quantification method and those studies were very time consuming and labour intensive. In this study a new line transect method, counting three transects of 504 points each (Robson et al., 2014), using the ×20 objective, was devised and tested to quantify macerals as defined by the ICCP standard classification system. Twelve points, 50 μm apart, were counted per field of view (600 μm). Tests on variation around the mean percentage inertinite with different numbers of points counted showed that, for 500 points, fluctuations are limited to within ±0.60%. The new method is less time-consuming allowing for more samples to be studied, and it accounts for variation in inertinite particle size and distribution through the *in situ* pillar. Crucially, the method used is comparable with previous work and industry methodologies. The same counting method was applied to crushed samples but only one transect of 504 points was counted due to the smaller size of the sample and the lack of stratigraphic information (e.g. bedding) preserved. The same ±0.60% uncertainty applies to all counts.

To facilitate comparison with previous work, where counting methods are often not stated, tests were undertaken using different counting methods (Whipple grid, Kötter graticule, Cross hairs). These tests revealed that there can be up to 5% variation between inertinite percentages obtained from identical transects using the different methods. This potential variation is taken into account when comparing new Schöningen results with those from the Glasspool and Scott (2010) database.

This work uses complete seams (either in their entirety for thinner seams or in parts for thick seams) to obtain overall fire activity, a measure that allows comparison with the database of Glasspool and Scott (2010); we are not addressing fire frequency here. However it should be borne in mind that both, high and low fire frequencies could yield the same 'seam-average' and 'part seam average' inertinite percentages.

4. Results

4.1. Crushed samples

The most common inertinite maceral is inertodetrinite (Fig. 2C and E), followed by semifusinite (Fig. 2B and D). Fusinite (Fig. 2A–C) and funginite (Fig. 2F) are the least common sub-macerals. Other than noting the occurrence of some large particles, inertinite size range and distribution cannot be addressed in crushed samples. There is no clear relationship between inertinite percentages or percentages of the huminite macerals, attrinite, textinite and ulminite (maceral data in supplementary spreadsheet pages 1 + 3).

Crushed samples representing the whole seam contain 1%–15% charred material (Fig. 3. Supplementary spreadsheet page 6). Both sample areas reveal high inertinite in seams Main–2 (average 13%, Fig. 3A and C), varied in seam 3 (4%–9%), low in seam 4 (average 1.5%), high in seam 5 (average 12%) and low in seams 6 to 9 (average 4%).

Crushed samples from part seams show that the variation within some seams is as high as the variation between seams (Fig. 3B and D). As might be expected, there is more spatial and temporal variation in inertinite in thick seams (Main, 1, 2, 6, 8, 9 range 2%–21%) than in thin seams (3, 4, 5, L, 7 range 1%–15%). In one set of part seam samples from thick seam 6, inertinite content varies by 17% (2–19%, Fig. 3B) but in another it varies by only 2% (4–6%, Fig. 3D). In one set of part seam samples from thin seam L, inertinite content does not vary (both 2%, Fig. 3B). In seams with overall high inertinite percentages, some part seam samples have percentages that are as low as those in the low inertinite content seams (4, L–9). The opposite is not observed; none of the part seam samples in low inertinite content seams (seam 4, 4%; seam L, 2% seam 7, 6%; seam 8, 5% seam 9, 8%; Fig. 3B and D) reach the high values of the high inertinite content seams (Main–2, 5 all contain beds with >12% inertinite). In summary, high inertinite content seams have both higher mean percentages and also larger variability. Therefore, two striking features are revealed by the novel examination of whole seam and part seam samples. First, a long-term overall decrease in inertinite percentages is visible from Main seam to seam 9. Second, imposed on this trend, are dramatic fluctuations in charcoal percentages between seams, but even more dramatically, within individual seams.

4.2. In situ pillars

Semifusinite (Fig. 2B and D centre) is the most common maceral in all pillars and inertodetrinite (Fig. 2C and E) is the second most common. Fusinite (Fig. 2A, C and D right) is uncommon in the Schöningen samples and funginite (Fig. 2F) is the least common maceral, although funginite percentages increase relative to other macerals in the samples from the younger seams L, 7, 8 and 9. Discrete bedding planes covered with charcoal (seams 5 and 6) and large (≥ several mm) charcoal particles distributed in discrete layers and lenses (Main seam and seam 1) which were observed in the field were interpreted as indicating intermittent fire activity by Riegel et al. (2012). Inertinite particles of different shapes and sizes are randomly distributed (Fig. 2C) in the majority of Schöningen material. However, some pillars contain areas with high proportions of inertodetrinite particles (Fig. 2E) and laterally discontinuous charcoal horizons.

Individual pillars contain 2%–19% charred material (Fig. 4A), a slightly larger range of values than those recorded in whole seam crushed samples (1%–15%). Inertinite percentages are high in seams Main–1 (average 15%), low in seams 3–4 (average 4.5%), higher in seams 5–6 (average 11%) and low in seams L–9 (average 3.5%).

4.3. Macerations

Charcoal abundance within macerated samples was estimated using a semi-quantitative modified ACFOR Domin scale from common to rare (Fig. 4B). The score of zero for seam 3 is explained by the absence of particles greater than 250 μm in that seam. The overall pattern of charcoal distribution through the succession is similar to that in the *in situ* pillars (Fig. 4A) and crushed samples (Fig. 3). The highest abundances occur in seams Main and 5 with the lowest abundances in seams L–9.

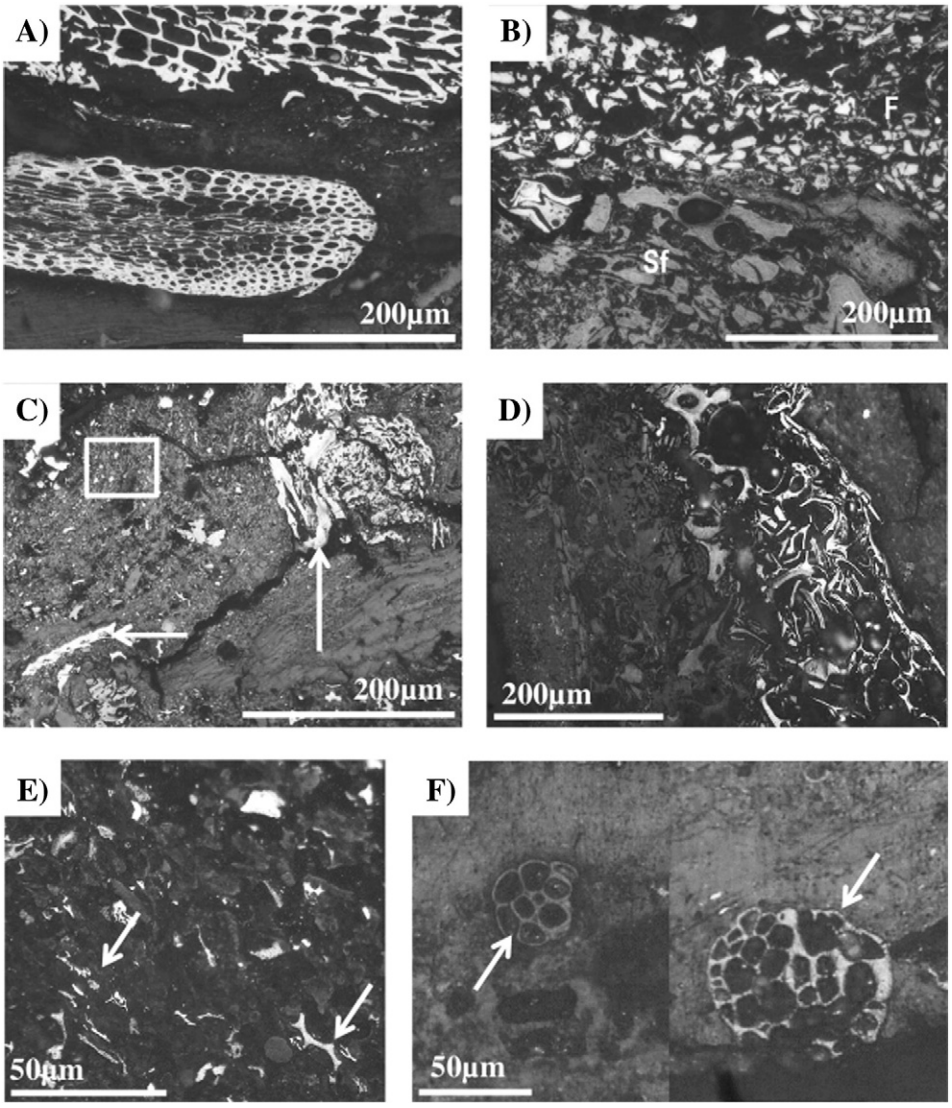

Fig. 2. Representative petrographic images to demonstrate the variety of inertinite (charcoal) macerals recorded from Schöningen lignites. Images obtained under oil using a reflectance microscope. (A) Fusinite particles with well preserved cellular structure. Large particles of local origin. (B) A large semifusinite (Sf) and fusinite (F) particle. (C) Fusinite particles (arrows) and inertodetrinite particles (box) in an attrinite/textinite matrix. (D) Partially charred particle (dark grey textinite on the left, pale grey semifusinite in the centre and white fusinite on the right) shows that not all material charred equally in Schöningen wildfires. (E) Inertodetrinite with remnants of cellular structure (arrows), likely evidence of regional wildfire activity. (F) Fungal sclerotia; uncharred (left) and charred (funginite) (right). (A & B seam 6, D seam 5, E & F seam 1, all from pillars; C crushed sample seam 1).

5. Discussion

5.1. Value of combined approaches for the study of charcoal

Different information can be obtained by various methods of studying charcoal but there are caveats applicable to each method. By choosing a specific size faction (250 µm–500 µm in this study), comparison of charcoal abundance between macerated samples is easier, although results can be misleading when a sample consists solely of small charcoal (seam 3, Fig. 4B). Low temperature charcoals with low lustre can be hard to recognise in macerated samples using light microscopy. By contrast, petrographic study of inertinite, in polished blocks or *in situ* pillars, can identify charcoal across a wide range of charring temperatures (e.g. fusinite/semifusinite) (Glasspool and Scott, 2013).

Due to the preparation method, crushed samples and macerated samples preserve no temporal or spatial distribution data and only a restricted perspective on particle size. In contrast, *in situ* pillars retain evidence of charcoal particle size and distribution (e.g. banded, clumped or irregular).

However, sampling constraints mean that *in situ* pillars only represent part of the seam, and therefore a limited window of fire activity, whereas a crushed sample can represent either the whole seam or part of it. Inertinite relative abundance in a high-resolution (every c. 5 cm) study using crushed samples of seam 1 (Inglis et al., in press) largely matches the lower resolution (part seam) results herein (Fig. 3B), with higher percentages at the top and lower percentages at the base of the seam. This indicates that inertinite variation can be adequately documented by lower resolution sampling.

There are benefits and limitations to each individual method. The combined study of *in situ* pillars, crushed samples and macerated samples provides a powerful tool for analysis of charcoal.

5.2. Inertinite macerals, size and distribution: wildfire implications

A mix of particle sizes from >500 µm to less than 10 µm (Fig. 2A, B, D, E) is visible in the *in situ* pillars. This indicates that the Schöningen material is a record of local wildfire activity (Innes and Simmons, 2000; Nichols et al., 2000) as well as regional activity (Scott and Glasspool, 2007; Scott, 2010). Semifusinite and inertodetrinite are the most common inertinite macerals quantified using both *in situ* pillars and crushed samples. Since inertodetrinite is considered to be predominantly wind-

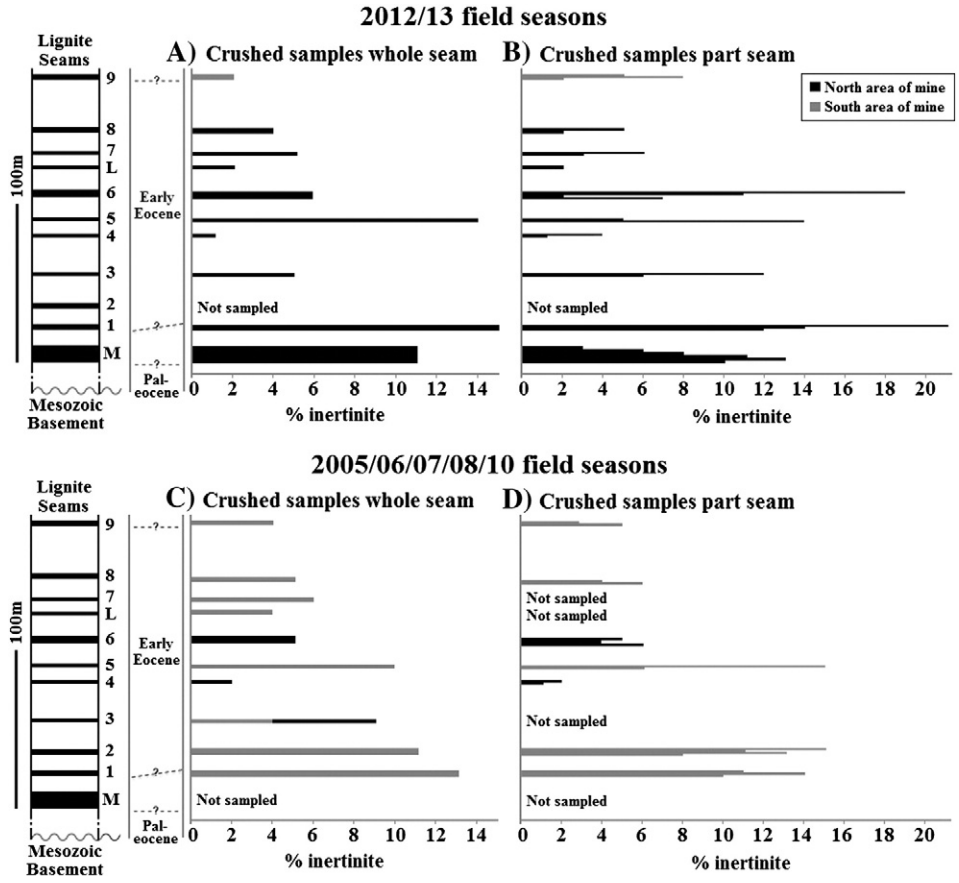

Fig. 3. Inertinite (charcoal) percentages from 11 seams at Schöningen, adjacent to simplified log (with seams to scale) adapted from Riegel et al. (2012). Uncertainty of 0.60% applies to all values (see Section 3.3). (A & C) Average total inertinite percentages in crushed samples representative of a whole seam. Due to the thickness of Main seam and seam 6, and the nature of access in the mine in 2012–2013, the two seams were collected as upper and lower portions and the inertinite percentages averaged (Main seam 9%–12%, seam 6 2%–11%). In 2005–2010 seam 3 was sampled in both areas of the mine. Seam L was sampled twice in the same area and results averaged (values 3% and 5%. (B and D) Total inertinite percentages in crushed samples representing parts of seams. Individual parts of seams can contain higher or lower inertinite percentages than the whole seam sample but seams 4 and L–9 never contain more than 8% inertinite. Although inertinite content is variable, both whole and part seam samples, collected from two areas of the mine in different field seasons, show a similar pattern, with higher inertinite percentages in Main seam, seams 1,2 and 5 and lower inertinite in seam 4 and in the later part of the Early Eocene (seams L–9).

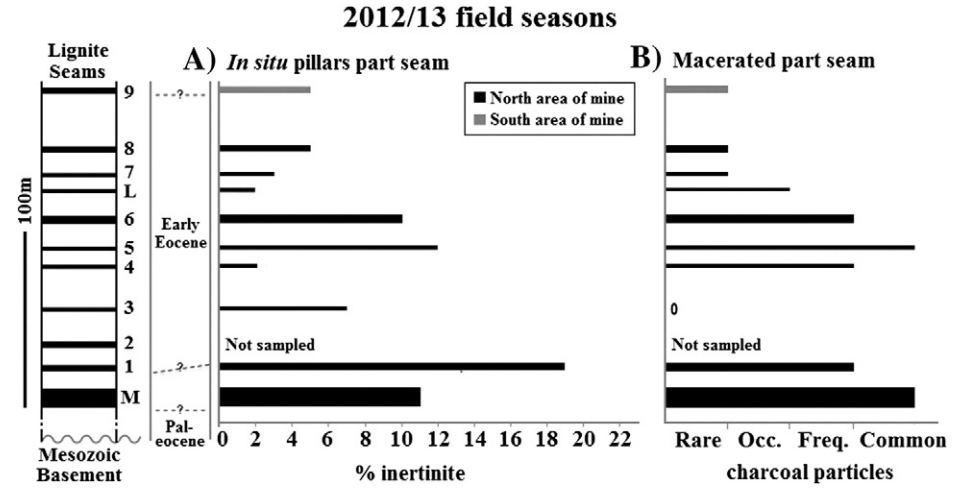

Fig. 4. Inertinite (charcoal) percentages from *in situ* pillars and charcoal abundance from macerated samples from Schöningen, adjacent to simplified log (with seams to scale) adapted from Riegel et al. (2012). (A) Inertinite (charcoal) percentages obtained from *in situ* pillars. Uncertainty of 0.60% applies to all values (see Section 3.3) and the maximum error on the mean is an additional ±0.24% (refer to supplementary spreadsheet page 4 for individual values for each pillar). Due to the thickness of Main seam and seam 6 and the nature of access in the mine, pillars were collected from the upper and lower parts of the seam and results were averaged (Main seam 6%–23%, seam 6 1%–18%). (B) Charcoal particles, released from samples representing the same bed as the *in situ* pillars, relative abundance estimated using a semi-quantitative method (modified ACFOR Domin scale). The 250 μm–500 μm size fraction was chosen as it is most likely to represent mainly local wildfire. The pattern of charcoal relative abundance from both methods is very similar to those shown in Fig. 3A and C.

blown due to its small size (Scott, 2010), it can be used as an indicator of local and regional high temperature crown fire activity (Clark, 1988; Clark et al., 1998; Scott, 2010). *In situ* pillars contain all particle sizes as all macerals are preserved in their original spatial and temporal context. The single plane of section studied might mean that some particles were cut at an angle or in a position that did not reflect their maximum size, but the effects would be minimal in this study of three transects in each pillar.

Inertinite in *in situ* pillars shows no distinctive distribution pattern unlike the repeated, multiple scale banding that characterises immediately pre-PETM fires at Cobham, UK (Collinson et al., 2007, 2009). At Schöningen inertinite is mostly irregularly distributed in polished pillars, with the occasional discontinuous band in some seams. This relative homogeneity may explain why pillars representing part of a seam (Fig. 4A) show a similar inertinite distribution pattern to that in crushed samples representing whole seams (Fig. 3A).

Areas of rare inertinite suggest that fuel would have accumulated between periods of fire activity, much as it does in modern fire prone areas (Pierce et al., 2004). Partially charred particles (Fig. 2D) in the *in situ* pillars indicate a brief heating duration or high levels of fuel moisture (Hudspith et al., 2012; Marynowski et al., 2014) as might be expected for wildfires in peat-forming settings.

5.3. Early Paleogene charcoal from Schöningen and the global Phanerozoic charcoal record

The high (11–19%, Figs. 3A, C and 4A) early Paleogene levels of inertinite (charcoal) in some seams at Schöningen are low by comparison with periods of mid to high fire activity recorded for intervals in the Paleozoic and Mesozoic by Glasspool and Scott (2010) i.e. the Permian = mean 44.4%, Late Jurassic = mean 26.1%, Middle Cretaceous = mean 42.8%. These high inertinite levels in the Paleozoic and Mesozoic are thought to be a consequence of higher atmospheric oxygen content which enabled wetter plant material to burn more easily (Glasspool and Scott, 2010). In the early Paleogene, models suggest that atmospheric oxygen levels began to stabilise to modern levels, so the effects of precipitation on wildfires may have increased (Belcher et al., 2013; Scott et al., 2014). Consequently, in spite of the overall warm early Paleogene climate, fire activity was reduced compared to that in the Paleozoic and Mesozoic.

Data from the three early Paleogene bins (Middle to Late Paleocene; Early Eocene; Middle to Late Eocene) in the Glasspool and Scott (2010) database, were re-plotted and Schöningen whole seam crushed sample results were superimposed upon them (Fig. 5). The Schöningen Main seam and seam 1 may be either earliest Eocene or latest Paleocene (Section 2.2) but for simplicity Fig. 5 shows their charcoal abundance superimposed on the Late Paleocene bin. Seam 9 is treated here as late Early Eocene (Section 2.2).

The database compiled by Glasspool and Scott (2010) displayed a stepped reduction in inertinite percentages from the middle Cretaceous (mean 42.8%) to the present day (mean 4.5%). The Middle to Late Paleocene bin has high inertinite percentages (mean 17%), the Early Eocene bin has lower inertinite percentages (mean 8.6%) and the Middle to Late Eocene bin has lower percentages still (mean 3.5%). When Main seam and seam 1 are treated as Paleocene (Fig. 5), inertinite percentages from Schöningen are slightly lower than mean values previously reported for the Paleocene to Paleocene–Eocene transition interval. Using the alternative age model, where all seams are Early Eocene, the high inertinite percentages for Main seam and seam 1 are higher than previously reported for the earliest Eocene.

Subsequently the inertinite percentages from Schöningen differ from those in Glasspool and Scott (2010), irrespective of possible alternative stratigraphic interpretations for seam 9. Inertinite percentages fall in seams 3 and 4, with seam 4 differing significantly from Glasspool and Scott's (2010) dataset (Fig. 5). Seam 4 palynology shows an increase in palm pollen (Riegel et al., 2012) compared to all

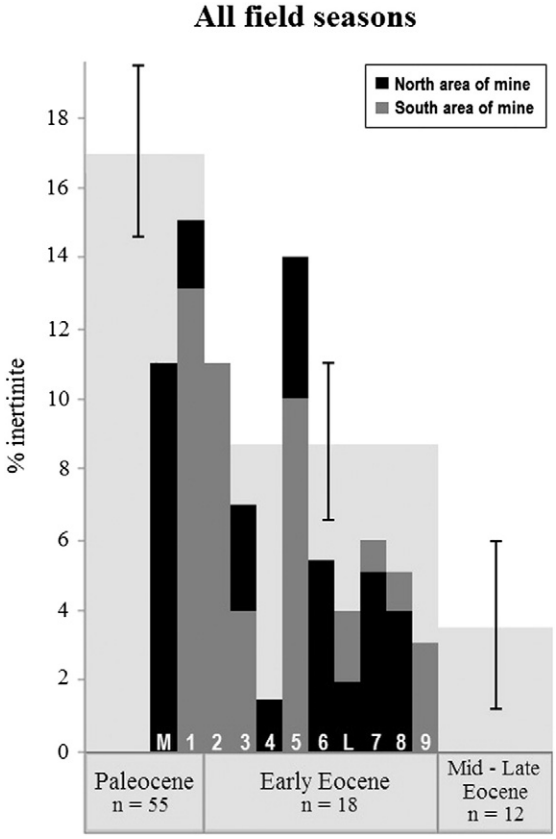

Fig. 5. Schöningen inertinite (charcoal) in crushed samples representing the whole of a seam (2005–2013 field seasons) presented in the context of the Glasspool and Scott (2010) database (pale grey background area with black bars showing 5% variation to account for different quantification methods (see Section 3.3)). Where samples were collected from the same area of the mine in different field seasons, the inertinite percentages were averaged (seams 3, 5%–9%; seam 4, 1%–2%; seam 6, 5%–6%; seam 9, 2%–4%). Schöningen inertinite percentages from Main seam and seam 1 are high, consistent with data from the Glasspool and Scott (2010) database for the Paleocene. Inertinite percentages remain high in the early Early Eocene (seam 2) but fall to a very low value (seam 4), and then rise again in the middle of the Early Eocene (seam 5). Subsequently, (seams 6–9) later Early Eocene inertinite percentages fall to values similar to those of the Middle and Late Eocene as reported by Glasspool and Scott (2010).

other seams. This might imply that local vegetation was less flammable, however low inertinite values also occur higher in the Schöningen sequence where there are typical palynological (Riegel et al., 2012) and huminite maceral assemblages (maceral data in supplementary spreadsheet pages 1 and 3). High inertinite percentages characterise seam 5 in the middle Early Eocene (possibly at the time of the EECO). These higher abundances are followed in the middle Early Eocene by a fall in inertinite in seams L–9 to low percentages characteristic of those reported for the Middle Eocene at Helmstedt (and other sites, unpublished Diploma thesis, Bode, 1994, University of Göttingen—Riegel et al., 1999, 2012), later Cenozoic records (Glasspool and Scott, 2010) and modern peat forming environments (Eble and Grady, 1993; Scott et al., 2014) the average being ~4.3%.

An increase in peat accumulation rates could result in a decrease in inertinite percentages but without any change in fire activity. This possibility is very unlikely to explain the decrease in inertinite percentages in seams L–9 at Schöningen because increased peat growth (hence higher peat accumulation rate) is more likely during accumulation of seams Main to 6 when climates were equally wet and included the warmest intervals (Section 5.4). Furthermore, this explanation is very unlikely to account for the sustained lower percentages of inertinite through the remaining Cenozoic, a time of climate cooling (Zachos et al., 2008).

Today, only lowland tropical rain forests and montane rain forests with an annual precipitation of 2000–3000 mm, evenly distributed over the year, are inflammable despite high thunderstorm activity (Goldammer, 1993). High precipitation and humidity have been inferred for the Middle Eocene in Central Europe (Riegel, 2001), allowing tropical elements to be sustained in the vegetation even though the climatic optimum had already passed. This suggests that low inertinite in seams L–9 may be linked to uninterrupted highly per-humid conditions preventing the flammability of forest litter.

The varied inertinite pattern at Schöningen suggests that fire activity fluctuated in the warmest parts of the Early Eocene (including high and low levels) before reaching consistently low levels from the mid to late Early Eocene onwards. The Schöningen data indicate that the transition to the modern low fire world occurred earlier than previously thought i.e. in the mid–late part of the Early Eocene, not in the Middle Eocene. Furthermore, the long term Cenozoic trend of falling inertinite levels (Glasspool and Scott, 2010) is supported by the data from Schöningen. This is evidence against any major influence of sampling bias in the Cenozoic part of the Glasspool and Scott (2010) global dataset.

5.4. Climate effects on early Paleogene wildfire

Models suggest that atmospheric oxygen fell to modern levels (21%) in the Early Eocene (Berner et al., 2003; Zachos et al., 2008; Berner, 2009). Oxygen is a key part of the wildfire triangle (Scott, 2000) with fire in wet vegetation unsustainable at atmospheric oxygen levels lower than 23% (Scott et al., 2014). The stabilisation of oxygen levels in the Early Eocene heralded the first time in Earth's history when oxygen was not the controlling factor on wildfire (Scott et al., 2014); consequently the impact of precipitation (Belcher et al., 2013) and temperature on wildfire would have increased. Changes in lightning (due to increased CO_2, Belcher et al., 2010), temperature (Westerling et al., 2006; Marlon et al., 2009; Scott et al., 2014), fuel formation (Scott, 2000) and moisture (Dimitrakopoulos and Papaioannou, 2001) can all affect wildfire activity. Increased rainfall would lead to wetter fuel but also to increased plant growth, which, when coupled with increased temperatures, could increase the burn potential of biomes previously little affected by wildfire.

Global climate patterns from the Paleocene to the middle Early Eocene show a long term warming trend on which transient hyperthermals were superimposed (Zachos et al., 2008; Bijl et al., 2013). The Paleocene–Eocene thermal maximum (PETM) is one short-lived hyperthermal. It is marked by (i) a global increase in temperatures of ~5 °C (Dunkley Jones et al., 2013) and (ii) irregularities in the hydrologic cycle (Bowen et al., 2004; Sluijs et al., 2006; Tipple et al., 2011; Handley et al., 2012; Krishnan et al., 2014). Similarly, the warmest climates of the EECO (c. 49 Ma) were marked by high global temperatures and changes in global monsoonal activity that affected the distribution of precipitation (Huber and Goldner, 2012).

It is suggested that the intensity and distribution of precipitation changed as a result of Paleogene warming (Huber and Goldner, 2012), with greater moisture transport to high latitudes (Pagani et al., 2006) and increased precipitation at mid to high latitudes, as evidenced by *Azolla* blooms in the Arctic and Nordic seas as far south as Denmark (Barke et al., 2012). Some areas may also have experienced enhanced seasonal extremes (John et al., 2008). Plink-Björklund et al. (2014) suggested that extremes in the hydrological cycle were manifested as increased precipitation 'peakedness' in the subtropics and mid-latitudes during hyperthermals, where high intensity rainfall events were followed by drier intervals. A large scale arid/semi-arid, humid, arid/semi-arid pattern across the PETM is recognisable in clay rich sequences from Egypt (Khozyem et al., 2013), the Tethys and the Atlantic (Bolle and Adatte, 2000), continental flood-plain sediments in the Spanish Pyrenees (Schmitz and Pujalte, 2007) and complex sedimentological and isotopic changes in Tanzanian sediments (Handley et al., 2012), suggesting that variability in rainfall was not restricted to one locality.

Main seam to seam 5 at Schöningen, deposited during the warmest intervals of the early Paleogene (probably including the PETM and including the EECO according to the current age model), contains the highest charcoal relative abundances based on the new petrological evidence from crushed samples (Fig. 3) and *in situ* pillars (Fig. 4A). The variability in inertinite in seams 3 and 6 (Fig. 3B and D) may record transitional periods from higher wildfire activity (Main–2, 5) to lower wildfire activity (4, L–9), at least locally and possibly globally. This suggests that brief drier intervals, following wet periods with increased growth and fuel load, may have led to increased wildfire activity during the warmest climates of the Paleogene. One possible modern analogue for this effect is in the Amazon rainforest (Cochrane, 2003). High fuel loads and temperatures coupled with lower humidity in periods of drought caused by modern climate change have increased the number of high-intensity wildfires (Brando et al., 2014). It is therefore possible that, although wetter, the warmest climates of the Early Eocene could have been more fire prone than 'background' Eocene greenhouse conditions, hence the variation in charcoal abundance between seams Main to 9 at Schöningen (Fig. 5).

6. Conclusions

Petrological analysis of lignites using crushed samples and *in situ* pillars provides detailed quantitative documentation of inertinite (charcoal) abundance in the Schöningen lignites whilst allowing for comparability with previous work and industry standards. Large charcoal particles (≥500 μm) in the rooted autochthonous early Paleogene lignites at Schöningen are unlikely to have been washed in and therefore represent locally occurring wildfires. Small particles, such as inertodetrinite, which can be easily carried by the wind, may be derived from both local and regional fires. The most common inertinite macerals quantified using both methods are semi-fusinite and inertodetrinite. In spite of their varied advantages and disadvantages, all three methods of analysis (crushed samples, *in situ* pillars and macerations) show very similar patterns of relative charcoal abundance through the early Paleogene of Schöningen.

Despite the early Paleogene greenhouse climate, the highest charcoal percentages at Schöningen are low in comparison to those recorded in Paleozoic and Mesozoic intervals. By the Eocene, atmospheric oxygen had stabilised to modern levels, increasing the effect of precipitation on wildfire. The highest charcoal abundances and greater within seam variability occur during the warmest intervals of the Early Eocene which also experience episodic precipitation. In the subsequent cooler periods, low charcoal percentages are recorded which are similar to those of the later Cenozoic and present day, suggesting that the onset of the modern low-fire world began earlier than previously thought, in the later part of the Early Eocene (Ypresian).

Acknowledgments

The authors thank e.on for allowing access to the Schöningen mine and the miners that shared technical support as well as their canteen. We are indebted to Karin Schmidt (Forschungsinstitut und Naturmuseum Senckenberg, Frankfurt, Germany) and Olaf Lenz (TU Darmstadt, Institut für Angewandte Geowissenschaften, Germany) for vital help with field work, transport and travel arrangements; to Neil Holloway and Sharon Gibbons (Earth Sciences, Royal Holloway University of London) for pillar preparation and lab assistance; and to Jim Hower and Michelle Johnston (Center for Applied Energy Research, University of Kentucky) for preparing polished blocks containing crushed samples. This work was supported by the Natural Environment Research Council [NE/J008656/1] [NE/J008591/1]. ACS thanks the Leverhulme Trust for the award of an Emeritus Research Fellowship. RDP acknowledges the Royal Society Wolfson Research Merit Award.

Appendix A. Supplementary data

An overview of the lignite seams, stratigraphic logs and accompanying field images included within the supplementary material (Robson et al., Paleogene wildfires Schöningen supplementary material) provide full details on beds and pillar location within each seam studied at Schöningen for the 2012 and 2013 field season. The individual counts synthesised in Figs. 3–5 are provided in a supplementary spreadsheet (Robson et al., Paleogene wildfires Schöningen supplementary spreadsheet). Page 1, Crushed samples maceral percentages; Page 2, Crushed samples maceral group percentages; Page 3, *In situ* pillar maceral percentages; Page 4, *In situ* pillar maceral group percentages; Page 5, *In situ* pillar and crushed sample inertinite percentages; Page 6, Crushed sample inertinite data used in Figs. 3 and 5. This material will be available on the Royal Holloway University of London "Pure" portal—pure.rhul.ac.uk/portal. Supplementary data associated with this article can be found, in the online version, at http://dx.doi.org/10.1016/j.palaeo.2015.07.016.

References

Ahrendt, H., Köthe, A., Lietzow, A., Marheine, D., Ritzkowski, S., 1995. Lithostratigraphie, Biostratigraphie und radiometrische Datierungen des Unter-Eozäns von Helmstedt (SE-Niedersachsen). Z. Dtsch. Geol. Ges. 146, 450–457.

Barke, J., van der Burgh, J., van Konijnenburg-van Cittert, J.H.A., Collinson, M.E., Pearce, M.A., Bujak, J., Heilmann-Clausen, C., Speelman, E.N., van Kempen, M.M.L., Reichart, G.-J., Lotter, A.F., Brinkhuis, H., 2012. Coeval Eocene blooms of the freshwater fern *Azolla* in and around Arctic and Nordic seas. Palaeogeogr. Palaeoclimatol. Palaeoecol. 337–338, 108–119.

Belcher, C.M., Collinson, M.E., Scott, A.C., 2005. Constraints on the thermal energy released from the Chicxulub impact: new evidence from multi-method charcoal analysis. J. Geol. Soc. 162, 591–602.

Belcher, C.M., Mander, L., Rein, G., Jervis, F.X., Haworth, M., Glasspool, I.J., Hesselbo, S.P., McElwain, J.C., 2010. Increased fire activity at the Triassic/Jurassic boundary in Greenland due to climate-driven floral change. Nat. Geosci. 3, 426–429.

Belcher, C.M., Collinson, M.E., Scott, A.C., 2013. A 450-million-year history of fire. In: Belcher, C.M. (Ed.), Fire Phenomena and the Earth System: an Interdisciplinary Guide to Fire Science, First edition Wiley-Blackwell, Chichester, pp. 229–249.

Berner, R., 2009. Phanerozoic atmospheric oxygen: new results using the GEOCARBSULF model. Am. J. Sci. 309, 603–606.

Berner, R., Beerling, D., Dudley, R., Robinson, J., Wildman, R., 2003. Phanerozoic atmospheric oxygen. Annu. Rev. Earth Planet. Sci. 31, 105–134.

Bijl, P.K., Sluijs, A., Brinkhuis, H., 2013. A magneto and chemostratigraphically calibrated dinoflagellate cyst zonation of the early Palaeogene South Pacific Ocean. Earth Sci. Rev. 124, 1–31.

Bode, T., 1994. Untersuchungen zur Fazies und Genese der eozänen Helmstedter Braunkohlen im unteren Teil der Oberflözgruppe im Tagebau Helmstedt (Bezirk Braunschweig). Unpublished Diploma thesis, University of Göttingen 95 pp.

Bolle, M.P., Adatte, T., 2000. Palaeocene-early Eocene climatic evolution in the Tethyan realm: clay mineral evidence. Clay Miner. 36, 249–261.

Bond, W.J., 2015. Fires in the Cenozoic: a late flowering of flammable ecosystems. Front. Plant Sci. 5, 1–11 (article 749).

Bowen, G.J., Beerling, D.J., Koch, P.L., Zachos, J.C., Quattlebaum, T., 2004. A humid climate state during the Palaeocene/Eocene thermal maximum. Nature 432, 495–499.

Bowman, D.M.J.S., Balch, J.K., Artaxo, P., Bond, W.J., Carlson, J.M., Cochrane, M.A., D'Antonio, C.M., DeFries, R.S., Doyle, J.C., Harrison, S.P., Johnston, F.H., Keeley, J.E., Krawchuk, M.A., Kull, C.A., Marston, J.B., Moritz, M.A., Prentice, I.C., Roos, C.I., Scott, A.C., Swetnam, T.W., van der Werf, G.R., Pyne, S.J., 2009. Fire in the Earth system. Science 324, 481–484.

Brandes, C., Pollok, L., Schmidt, C., Wilde, V., Winsemann, J., 2012. Basin modelling of a lignite-bearing salt rim syncline: insights into rim syncline evolution and salt diapirism in NW Germany. Basin Res. 24, 699–716.

Brandes, C., Schmidt, C., Tanner, D.C., Winesmann, J., 2013. Paleostress pattern and salt tectonics within a developing foreland basin (north-western Subhercynian Basin, northern Germany). Int. J. Earth Sci. 102, 2239–2254.

Brando, P.M., Balch, J.K., Nepstad, D.C., Morton, D.C., Putz, F.E., Coe, M.T., Silvério, D., Macedo, M.N., Davidson, E.A., Nóbrega, C.C., Alencar, A., Soares-Filho, B.S., 2014. Abrupt increases in Amazonian tree mortality due to drought-fire interactions. Proc. Natl. Acad. Sci. U. S. A. 111, 6347–6352.

Clark, J.S., 1988. Particle motion and the theory of charcoal analysis: source area, transport, deposition, and sampling. Quat. Res. 30, 67–80.

Clark, J.S., Lynch, J., Stocks, B.J., Goldammer, J.G., 1998. Relationships between charcoal particles in air and sediments in west-central Siberia. The Holocene 8, 19–29.

Cochrane, M.A., 2003. Fire science for rainforests. Nature 421, 913–919.

Collinson, M.E., Steart, D.C., Scott, A.C., Glasspool, I.J., Hooker, J.J., 2007. Episodic fire, runoff and deposition at the Palaeocene-Eocene boundary. J. Geol. Soc. 164, 87–97.

Collinson, M.E., Steart, D.C., Harrington, G.J., Hooker, J.J., Scott, A.C., Allen, L.O., Glasspool, I.J., Gibbons, S.J., 2009. Palynological evidence of vegetation dynamics in response to palaeoenvironmental change across the onset of the Paleocene–Eocene thermal maximum at Cobham, Southern England. Grana 48, 38–66.

Costa, L.I., Manum, S.B., 1988. The Description of the Interregional Zonation of the Paleogene. In: Vinken, R. (Ed.), The North West European Tertiary Basin. Results of the International Geological Correlation Programme Project No 124. Geologisches Jahrbuch A100, pp. 321–330.

Dimitrakopoulos, A., Papaioannou, K.K., 2001. Flammability assessment of Mediterranean forest fuels. Fire. Technol 37, 143–152.

Dunkley Jones, T., Lunt, D.J., Schmidt, D.N., Ridgwell, A., Sluijs, A., Valdes, P.J., Maslin, M., 2013. Climate model and proxy data constraints on ocean warming across the Paleocene–Eocene thermal maximum. Earth Sci. Rev. 125, 123–145.

Eble, C.F., Grady, W.C., 1993. Palynologic and Petrographic Characteristics of Two Middle Pennsylvanian Coal Beds and a Probable Modern Analogue. In: Cobb, J.C., Cecil, C.B. (Eds.), Modern and Ancient Coal-Forming Environments. Geological Society of America Special Paper 286, pp. 119–138.

Fabbri, D., Torri, C., Simoneit, B.R.T., Marynowski, L., Rushdi, A.I., Fabianska, M.J., 2009. Levoglucosan and other cellulose and lignin markers in emissions from burning of Miocene lignites. Atmos. Environ. 43, 2286–2295.

Figueiral, I., 1999. Lignified and Charcoalified Fossil Wood. In: Jones, T.P., Rowe, N.P. (Eds.), Fossil Plants and Spores: Modern Techniques. Geological Society, London, pp. 92–96.

Glasspool, I.J., Scott, A.C., 2010. Phanerozoic concentrations of atmospheric oxygen reconstructed from sedimentary charcoal. Nat. Geosci. 3, 627–630.

Glasspool, I.J., Scott, A.C., 2013. Identifying Past Fire Events. In: Belcher, C.M. (Ed.), Fire Phenomena in the Earth System – An Interdisciplinary Approach to Fire Science. Wiley-Blackwel, Chichester, pp. 179–206.

Goldammer, J.G., 1993. Feuer in Waldökosystemen der Tropen und Subtropen. Birkhäuser Verlag, Basel, p. 251.

Gradstein, F.M., 2012. Introduction. In: Gradstein, F.M., Schmitz, M.D., Ogg, G.M. (Eds.), The Geologic Time Scale, First edition 2-volume set. Elsevier, Boston, pp. 1–30.

Guo, Y., Bustin, R.M., 1998. FTIR spectroscopy and reflectance of modern charcoal and fungal decyed woods: implications for studies of inertinite in coals. Int. J. Coal Geol. 37, 29–53.

Handley, L., O'Halloran, A., Pearson, P.N., Hawkins, E., Nicholas, C.J., Schouten, S., McMillan, I.K., Pancost, R.D., 2012. Changes in the hydrological cycle in tropical East Africa during the Paleocene–Eocene thermal maximum. Palaeogeogr. Palaeoclimatol. Palaeoecol. 329–30, 10–21.

Harris, T.M., 1958. Forest fire in the Mesozoic. J. Ecol. 46, 447–453.

Holden, J., 2005. Peatland hydrology and carbon release: why small-scale matters. Phil. Trans. R. Soc. A 363, 2891–2913.

Hower, J.C., O'Keefe, J.M.K., Watt, M.A., Pratt, T.J., Eble, C.F., Stucker, J.D., Richardson, A.R., Kostova, I.J., 2009. Notes on the origin of inertinite macerals in coals: observations on the importance of fungi in the origin of macrinite. Int. J. Coal Geol. 80, 135–143.

Huber, M., Goldner, A., 2012. Eocene monsoons. Asian Clim. Tectonics 44, 3–23.

Hudspith, V., Scott, A.C., Collinson, M.E., Pronina, N., Beeley, T., 2012. Evaluating the extent to which wildfire history can be interpreted from inertinite distribution in coal pillars: an example from the Late Permian, Kuznetsk Basin, Russia. Int. J. Coal Geol. 89, 13–25.

ICCP, 1963. International Committee for Coal Petrology. International Handbook of Coal Petrography. Centre National De La Recherche Scientifique, France.

ICCP, 2001. International Committee for Coal Petrology. The new inertinite classification (ICCP System 1994). Fuel 80, 459–471.

Inglis, G.N., Collinson, M.E., Wilde, V., Riegel, W., Lenz, O., Robson, B.E., Pancost, R.D., 2015. Ecological and biogeochemical change in an early Paleogene peat-forming environment: linking biomarkers and palynology. Palaeogeogr. Palaeoclimatol. Palaeoecol. (in press).

Innes, J.B., Simmons, I., 2000. Mid Holocene charcoal stratigraphy, fire history and palaeoecology at North Gill, North York Moors, UK. Palaeogeogr. Palaeoclimatol. Palaeoecol. 164, 151–165.

John, C.M., Bohaty, S.M., Zachos, J.C., Sluijs, A., Gibbs, S., Brinkhuis, H., Bralower, T.J., 2008. North American continental margin records of the Paleocene–Eocene thermal maximum: implications for global carbon and hydrological cycling. Paleoceanography 23 (PA2217).

Jones, T.P., Scott, A.C., Mattey, D.P., 1993. Investigations of "fusain transition fossils" from the Lower Carboniferous: comparisons with modern partially charred wood. Int. J. Coal Geol. 22, 37–59.

Jones, T.P., Chaloner, W.G., Kuhlbusch, T.A.J., 1997. Proposed Bio-Geological and Chemical Based Terminology for Fire-Altered Plant Matter. In: Clark, J.S., Cachier, H., Goldammer, J.G., Stocks, B. (Eds.), Sediment Records of Biomass Burning and Global ChangeNATO ASI Series I: Global Environmental Change vol. 51. Springer, Verlag Berlin Heidelberg, pp. 10–22.

Khozyem, H., Adatte, T., Spangenberg, J.E., Tantawy, A.A., Keller, G., 2013. Palaeoenvironmental and climatic changes during the Palaeocene–Eocene thermal maximum (PETM) at the Wadi Nukhul Section, Sinai, Egypt. J. Geol. Soc. Lond. 170, 341–352.

Komarek, E.V., 1972. Ancient Fires. Proceedings of the Annual Tall Timbers Fire Ecology Conference. 12, pp. 219–240.

Köthe, A., 1990. Paleogene dinoflagellates from Northwest Germany. Biostratigraphy and paleoenvironment. Geol. Jahrb. A118, 3–111.

Köthe, A., 2012. A revised Cenozoic dinoflagellate cyst and calcareous nannoplankton zonation for the German sector of the southeastern North Sea Basin. Newsl. Stratigr. 45, 189–220.

Krishnan, S., Pagani, M., Huber, M., Sluijs, A., 2014. High latitude hydrological changes during the Eocene thermal maximum 2. Earth Planet. Sci. Lett. 404, 167–177.

Krutzsch, W., 2011. Stratigrafie und Klima des Paläogens im mitteldeutschen Ästuar im Vergleich zur marinen nördlichen Umrahmung. Z. Dtsch. Ges. Geowiss. 162, 19–47.

Lenz, O.K., 2005. Palynologie und Paläoökologie eines Küstenmoores aus dem Mittleren Eozän Mitteleuropas—Die Wulfersdorfer Flözgruppe aus dem Tagebau Helmstedt, Niedersachsen. Palaeontographica B 271, 1–157.

Manger, G., 1952. Der Zusammenhang von Salztektonik und Braunkohlenbildung bei der Entstehung der Helmstedter Braunkohlenlagerstätten. Mitteilungen aus dem Geologischen Staatsinstitut in Hamburg 21 pp. 7–45.
Marlon, J., Bartlein, P.J., Walsh, M.K., Harrison, S.P., Brown, K.J., Edwards, M.E., Higuera, P.E., Power, M.J., Anderson, R.S., Briles, C., Brunelle, A., Carcaillet, C., Daniels, M., Hu, F.S., Lavoie, M., Long, C., Minckley, T., Richard, P.J.H., Scott, A.C., Shafer, D.S., Tinner, W., Umbanhowar, C.E., Whitlock, C., 2009. Wildfire responses to abrupt climate change in North America. Proc. Natl. Acad. Sci. 106, 2519–2524.
Marynowski, L., Kubik, R., Uhl, D., Simoneit, B.R.T., 2014. Molecular composition of fossil charcoal and relationship with incomplete combustion of wood. Org. Geochem. 77, 22–31.
McParland, L.C., Collinson, M.E., Scott, A.C., Steart, D.C., Grassineau, N.V., Gibbons, S.J., 2007. Ferns and fires: experimental charring of ferns compared to wood and implications for paleobiology, paleoecology, coal petrology and isotope geochemistry. Palaios 22, 528–538.
Moore, T.C., Shearer, J.C., 2003. Peat/coal type and depositional environment — are they related? Int. J. Coal Geol. 56, 233–252.
Moore, T.A., Shearer, J.C., Miller, S.L., 1996. Fungal origin of oxidised plant material in the Palangkaraya peat deposit, Kalimantan Tengah, Indonesia: implications for inertinite formation in coal. Int. J. Coal Geol. 30, 1–23.
Nichols, G., 1999. Sedimentology and Stratigraphy. Blackwell Science, London, p. 355.
Nichols, G.J., Cripps, J.A., Collinson, M.E., Scott, A.C., 2000. Experiments in waterlogging and sedimentology of charcoal: results and implications. Palaeogeogr. Palaeoclimatol. Palaeoecol. 164, 43–56.
Osman, A., Pollok, L., Brandes, C., Winsemann, J., 2013. Sequence stratigraphy of a Paleogene coal bearing rim syncline: interplay of salt dynamics and sea—level changes, Schöningen, Germany. Basin Research 25, 675–708.
Pagani, M., Pedentchouk, N., Huber, M., Sluijs, A., Schouten, S., Brinkhuis, H., Sinninghe Damste, J.S., Dickens, G.R., the Expedition 302 Scientists, 2006. Arctic hydrology during global warming at the Palaeocene/Eocene thermal maximum. Nature 442, 671–675.
Pancost, R.D., Steart, D.S., Handley, L., Collinson, M.E., Hooker, J.J., Scott, A.C., Grassineau, N.V., Glasspool, I.J., 2007. Increased terrestrial methane cycling at the Palaeocene-Eocene thermal maximum. Nature 449, 332–335.
Pausas, J.G., Keeley, J.E., 2009. A burning story: the role of fire in the history of life. Bioscience 59, 593–601.
Pflug, H.D., 1952. Palynologie und Stratigraphie der eozänen Braukohlen von Helmstedt. Paläontol. Z. 26, 112–137.
Pierce, J.L., Meyer, G.A., Jull, A.J.T., 2004. Fire-induced erosion and millennial-scale climate change in northern ponderosa pine forests. Nature 432, 87–90.
Plink-Björklund, P., Birgeneier, L., Jones, E., 2014. Extremely bad early Eocene weather: evidence for extreme precipitation from river deposits. Rend. Online Soc. Geol. Ital. 31, 175–176.
Potonié, R., 1929. Spuren von Wald- und Moorbränden in Vergangenheit und Gegenwart. Jahrb. Preuss. Geol. Landesanst. 49 (for 1928), 1184–1203.
Riegel, W., 2001. Die Geiseltalkohle im Rahmen der Braunkohlenlagerstätten des mitteleuropäischen Tertiärs. Hallesches Jahrbuch für Geowissenschaften B, Beiheft 13 pp. 41–47.
Riegel, W., Bode, T., Hammer, J., Hammer-Schiemann, G., Lenz, O., Wilde, V., 1999. The palaeoecology of the Lower and Middle Eocene at Helmstedt, Northern Germany – a study in contrasts. Acta Palaeobot. (Supplement 2), 349–358.
Riegel, W., Wilde, V., Lenz, O.K., 2012. The early Eocene of Schöningen (N-Germany) – an interim report. Aust. J. Earth Sci. 105, 88–109.
Riegel, W., Lenz, O.K., Wilde, V., 2015. From open estuary to meandering river in a greenhouse world: an ecological case study from the middle Eocene of Helmstedt, northern Germany. Palaios 30, 304–326.
Robson, B.E., Collinson, M.E., Riegel, W., Wilde, V., Scott, A.C., Pancost, R.D., 2014. A record of fire through the Early Eocene. Rend. Online Soc. Geol. Ital. 31, 187–188.
Schmitz, B., Pujalte, V., 2007. Abrupt increase in seasonal extreme precipitation at the Paleocene–Eocene boundary. Geology 35, 215–218.
Scott, A.C., 1989. Observations on the nature and origin of fusain. Int. J. Coal Geol. 12, 443–475.
Scott, A.C., 1991a. Coal: Its origin and future. Teach. Earth Sci. 16, 24–36.
Scott, A.C., 1991b. An introduction to applications of palaeobotany and palynology to coal geology. Bull. Soc. Geol. Fr. 162, 145–153.
Scott, A.C., 2000. The pre-Quaternary history of fire. Palaeogeogr. Palaeoclimatol. Palaeoecol. 164, 281–329.
Scott, A.C., 2010. Charcoal recognition, taphonomy and uses in palaeoenvironmental analysis. Palaeogeogr. Palaeoclimatol. Palaeoecol. 291, 11–39.
Scott, A.C., Glasspool, I.J., 2007. Observations and experiments on the origin and formation of inertinite group macerals. Int. J. Coal Geol. 70, 53–66.
Scott, A.C., Cripps, J.A., Collinson, M.E., Nichols, G.J., 2000. The taphonomy of charcoal following a recent heathland fire and some implications for the interpretation of fossil charcoal deposits. Palaeogeogr. Palaeoclimatol. Palaeoecol. 164, 1–31.
Scott, A.C., Pinter, N., Collinson, M.E., Hardiman, M., Anderson, R.S., Brain, A.P.R., Smith, S.Y., Marone, F., Stampanoni, M., 2010. Fungus, not comet or catastrophe, accounts for carbonaceous spherules in the Younger Dryas "impact layer". Geophys. Res. Lett. 37, L14302.
Scott, A.C., Bowman, D.M.J.S., Bond, W.J., Pyne, S.J., Alexander, M.E., 2014. Fire on Earth: An Introduction. First edition. Wiley-Blackwell, Chichester.
Sluijs, A., Schouten, S., Pagani, M., Woltering, M., Brinkhuis, H., Sinninghe Damsté, J.S., Dickens, J.R., Huber, M., Reichart, G.J., Stein, R., Matthiessen, J., Lourens, L.J., Pedentchouk, N., Backman, J., Moran, K., the Expedition 302 Scientists, 2006. Subtropical Arctic Ocean temperatures during the Palaeocene/Eocene thermal maximum. Nature 441, 610–613.
Standke, G., 2008. Paläogeografie des älteren Tertiärs (Paläozän bis Untermiozän) im mitteleuropäischen Raum. Z. Dtsch. Ges. Geowiss. 159, 81–103.
Sýkorová, I., Pickel, W., Christanis, K., Wolf, M., Taylor, G.H., Flores, D., 2005. Classification of huminite – ICCP System 1994. Int. J. Coal Geol. 62, 85–106.
Taylor, G.H., Teichmüller, M., Davis, A., Diessel, C.F.K., Littke, R., Robert, P., 1998. Organic Petrology. First edition. Gebrüder Borntraeger, Berlin, Stuttgart.
Teichmüller, M., 1989. The genesis of coal from the viewpoint of coal petrology. Int. J. Coal Geol. 12, 1–87.
Tipple, B.J., Pagani, M., Krishnan, S., Dirghangi, S.S., Galeotti, S., Agnini, C., Giusberti, L., Rio, D., 2011. Coupled high-resolution marine and terrestrial records of carbon and hydrologic cycles variations during the Paleocene–Eocene Thermal Maximum (PETM). Earth Planet. Sci. Lett. 311, 82–92.
Valentim, B., Hower, J.C., O'Keefe, J.M.K., Rodrigues, S., Ribeiro, J., Guedes, A., 2013. Notes on the origin of altered macerals in the Ragged Edge of the Pennsylvanian (Asturian) Herrin coalbed, Western Kentucky. Int. J. Coal Geol. 115, 24–40.
Vaughan, A.V., Nichols, G., 1995. Controls on the deposition of charcoal—implications for sedimentary accumulations of fusain. J. Sediment. Res. A 65, 129–135.
Westerling, A.L., Hidalgo, H.G., Cayan, D.R., Swetnam, T.W., 2006. Warming and earlier spring increase Western U.S. forest wildfire activity. Science 313, 940–943.
Winston, R.B., 1993. Reassessment of the evidence for primary fusinite and degradofusinite. Organic Geochemistry 20, 209–221.
Wüst, R.A.J., Hawke, M.I., Bustin, R.M., 2001. Comparing maceral ratios from tropical peatlands with assumptions from coal studies: do classic petrographic interpretation methods have to be discarded? Int. J. Coal Geol. 48, 115–132.
Zachos, J.C., Dickens, G.R., Zeebe, R.E., 2008. An early Cenozoic perspective on greenhouse warming and carbon-cycle dynamics. Nature 451, 279–283.